XII International Conference on Computational Plasticity. Fundamentals and Applications
COMPLAS XII
E. Oñate, D.R.J. Owen, D. Peric and B. Suárez (Eds)

HYSTERETIC BEAM ELEMENT WITH DEGRADING BOUC-WEN MODELS

SOFIANOS CHRISTOS, KOUMOUSIS VLASIS

National Technical University of Athens (NTUA)
Institute of Structural Analysis & Aseismic Research
Zografou Campus, 15780, Athens, Greece.
email: sofianoschristos@yahoo.gr; vkoum@central.ntua.gr

Key words: Degrading elastoplastic models, hysteretic beam element.

Abstract. In this work a beam element based on the finite element method, suitable for the inelastic dynamic analysis of structures is presented. The hysteretic beam element proposed by Triantafyllou and Koumousis [1] is extended to account for stiffness degradation, strength deterioration and pinching phenomena. The behavior of the element is governed by the Bouc-Wen model of hysteresis while stiffness and strength degradation are based on Baber and Wen model [2] and pinching on Foliente's model [3]. The case of non-symmetrical yielding, important for concrete members, is also taken into account.

The proposed formulation is based on additional hysteretic degrees of freedom which herein are considered as hysteretic curvatures and hysteretic axial deformations of the cross-sections. The elements are assembled using the direct stiffness method to determine the mass and viscous damping matrices, as well as the elastic stiffness and the hysteretic matrix of the structure. The entire set of governing equations of the structure is solved simultaneously. This consists of the linear global equations of motion and the nonlinear local constitutive evolutionary equations for every element. The system is converted into a state space form and the numerical solution is obtained implementing a variable-order solver based on numerical differentiation formulas (NDFs). In this way linearization at the global structural level is avoided facilitating considerably the solution. Furthermore, degradation phenomena are easily controlled through the model parameters at the element level and not in a macroscopic way which requires a computationally demanding bookkeeping mechanism.

Numerical results are presented that validate the proposed formulation and verify its computational efficiency as compared to the standard elastoplastic finite element method and existing experimental data.

1 INTRODUCTION

Hysteresis is a phenomenon where a system's response depends not only on its current state but also on the history of previous states. It is a nonlinear phenomenon characterized as rate-independent. The phenomenon of hysteresis is manifested in various scientific fields ranging from Chemistry and Biology to Mechanics.

For many years the design and analysis of structures was based on the elastic method and allowable stresses. Its simplicity and low demand in computational resources offered the basis

for design in previous decades. This was followed by the Load Resistant Factor Design (LRFD) method also based on elastic analysis. These methods though fail to capture the real behavior of a structure especially under dynamic loading. Therefore the need for more refined models was evident. Several hysteretic models have been developed in the last decades. These can be divided into two main categories, the multi-segment hysteretic models and smooth hysteretic models.

Multi-segmental models, such as bilinear, trilinear and other multi-linear hysteretic models preceded the smooth models. These divide the behavior of the element into partial linear stages such as the initial elastic, yielding, hardening/softening stages with unloading and reloading branches. Examples of such models are those proposed by Clough (1966), Takeda (Takeda et al. 1970) [13] and Park (Park et al. 1987) [14] among others.

Alternatively, smooth hysteretic models are based on continuous change of stiffness after yield and during unloading stages, which can accommodate also degradation phenomena. They have the ability to model different types of hysteretic behavior and are based on a smooth hysteretic function and a set of user defined parameters. The Bouc-Wen model belongs to this category and has been widely used. Extensions of this model are the Baber – Noori (1985) [11], Baber – Wen (1981) [2], Foliente (1995) [3] and Sivaselvan-Reinhorn model (2000) [12].

2 THE BOUC-WEN HYSTERETIC MODEL

In this work the Bouc-Wen hysteretic model is employed. It is a smooth hysteretic model that was first proposed by Bouc (1967) and was later modified by Wen (1980)[4]. Its mathematical description for a Single Degree of Freedom (sdof) system is as follows:

$$\begin{cases} m\ddot{u} + c\dot{u} + aKu + z = p \\ \dot{z} = K\dot{u} \\ K = K\left(z, sgn\left(du\right)\right) = (1-a)K_0\left[A - \left|z\right|^n (\beta + \gamma sgn(zdu))\right] \end{cases} \tag{1}$$

where m, c, K are the mass, viscous damping and stiffness respectively and α is the ratio of the post-yield to the initial elastic stiffness: $\alpha=K_{pl}/K_{el}$.

According to Ma et al.[5] parameter A was considered to be equal to one, A=1. The signum function *sgn(x)* returns 1, 0, or -1 (depending on whether x is positive, zero, or negative, respectively).

The above formulation leads basically to a non-linear first order differential equation based on a set of parameters defined by the user. The hysteretic function z and its derivative with respect to time $\dot{z}$ are related to the derivative of displacements with respect to time $\dot{u}$ (namely the velocity), times a non-linear coefficient K, as shown in (1). The Bouc-Wen model can be visualized as a mechanical model consisting of a parallel combination of a linear spring with stiffness αK_{el} and a nonlinear spring with stiffness $(1-\alpha)K_{el}$ (Figure 1).

Considering a single degree of freedom system the restoring force is equal to the sum of the elastic force F^{el} and the hysteretic force F^h:

$$F\left(t\right) = a\frac{F_y}{u_y}u\left(t\right) + (1-a)\frac{F_y}{u_y}z\left(t\right) = F^{el}(t) + F^h(t) \tag{2}$$

Regarding the bending degrees of freedom (Figure 1) the generalized moment-curvature relation can be expressed as:

$$M(t) = aEI\varphi(t) + (1-a)EIz(t) \tag{3}$$

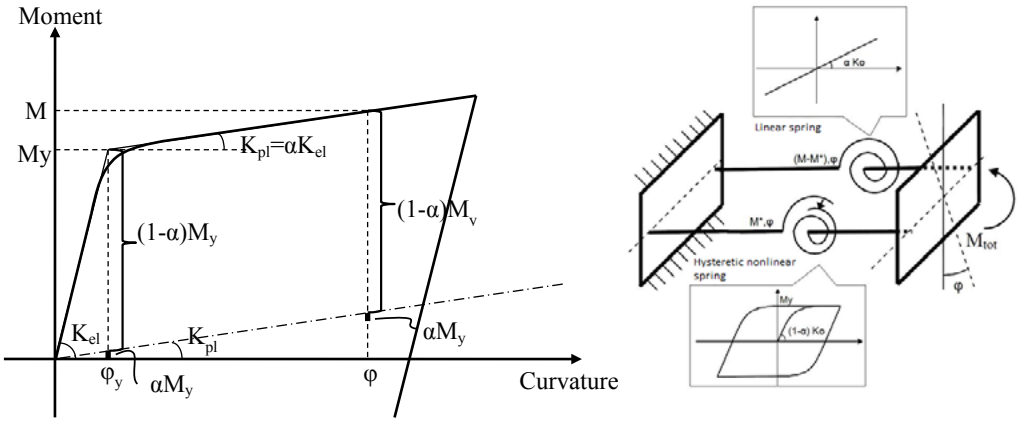

Figure 1: Bouc-Wen model expressed in Moment-Curvature terms and its mechanical model.

The hysteretic function *z(t)* is governed by the following non-linear first order differential equation:

$$\dot{z}(t) = \dot{u}\left[1 - \left|\frac{z}{z_y}\right|^n \left(\beta + \gamma sgn(z\dot{u})\right)\right] \tag{4}$$

The parameter *n* is a positive number that controls the transition from the elastic to the inelastic region. Larger values of *n* lead to sharper transition and the response approaches the bilinear behavior as shown in Figure 2:

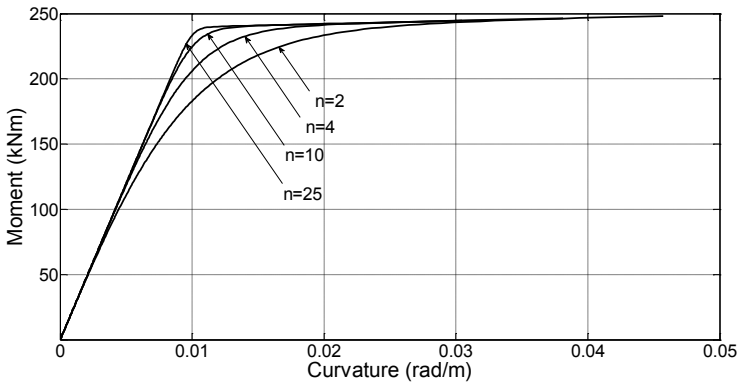

Figure 2: Response for different values of n.

3 HYSTERETIC BEHAVIOR WITH ASYMMETRIC YIELD MOMENT

To account for cross sections with asymmetric yield moments Wang and Foliente [6] proposed the following relation when considering bending degrees of freedom:

$$M_y^* = (1-a)\left[\left(\frac{1+sgn(M^*)}{2}\right)M_y^+ + \left(\frac{1-sgn(M^*)}{2}\right)M_y^-\right] \tag{5}$$

By expanding relation (5) for both the bending and axial degrees of freedom the following relation is derived:

$$z_y = \left[\left(\frac{1+sgn(z)}{2}\right)z_y^+ + \left(\frac{1-sgn(z)}{2}\right)z_y^-\right] \tag{6}$$

where z_y can be regarded as either the yield curvature or the yield centerline axial deformation. Using equation (6) the model is capable of simulating non symmetrical yielding which is important especially for concrete frames. An example of hysteretic loops produced with asymmetric yield moment is shown in Figure 3 where the positive yielding moment is less than 200 kNm while the negative is over 200 kNm for a frame cross section.

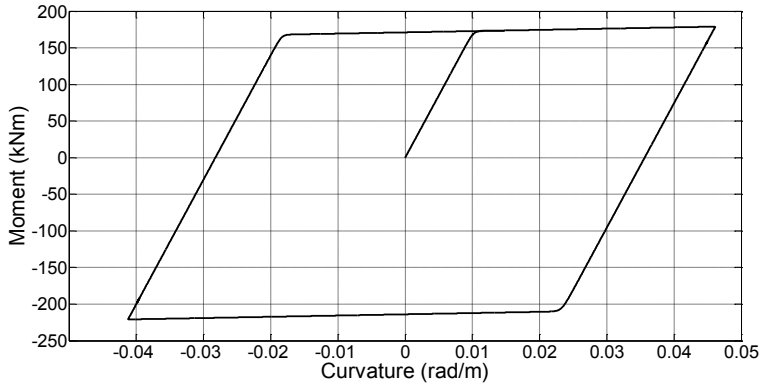

Figure 3: Hysteretic loops with asymmetric yield moment.

4 HYSTERETIC BEHAVIOR WITH DEGRADATIONS

Hysteretic loops presented in the previous figures don't fully describe the real behavior of structures subjected to cyclic loading. This is due to the fact that under cyclic loading the phenomena of stiffness degradation, strength deterioration and pinching are usually manifested. These are due to micro cracks being created and extended in later loading cycles, which lead to stiffness and strength loss. Pinching is the sudden loss of stiffness resulting in loops that are thinner in middle range than at the ends. It is caused by the slipping of reinforcement in reinforced concrete members or the loosening and slipping of joints in timber and steel structures. The models proposed by Baber and Wen (1981) [2] are employed in this paper for stiffness and strength degradation together with the one by Foliente (1995) [3] for pinching.

In their work Barber and Wen (1981) presented two additional parameters v_s and n_s to account for stiffness degradation and strength deterioration. These parameters where

introduced into the differential equation as follows:

$$\dot{z}(t)=\left\{1-v_s\left|\frac{z}{z_y}\right|^n(\beta+\gamma sgn(z\dot{\varphi}))\right\}\frac{\dot{\varphi}}{n_s} \tag{7}$$

where v_s is the parameter that controls the strength deterioration and n_s is the parameter controlling stiffness degradation. These two parameters are functions of the hysteretic energy dissipation (namely the energy dissipated by the hysteretic spring) and are defined by the following relations:

$$\begin{aligned} n_s &= 1+c_n e^h,\ \ c_n \geq 0 \\ v_s &= 1+c_v e^h,\ \ c_v \geq 0 \end{aligned} \tag{8}$$

The energy dissipated by the hysteretic spring is defined both for bending and axial degrees of freedom respectively as:

$$\begin{aligned} e^h &= \int (1-a)EIz(t)d\varphi \\ e_u^h &= \int (1-a)EAz_u(t)de \end{aligned} \tag{9}$$

The dissipated energy is represented by the area inscribed by the hysteretic loops. Parameters c_n and c_v are positive with usual values being in the order of 10^{-3}-10^{-4}. It results that for n_s=v_s=1 the model does not degrade. Figures 4(a) and 4(b) show the effect of varying the values of c_n and c_v respectively on a frame cross section under sinusoidal excitation.

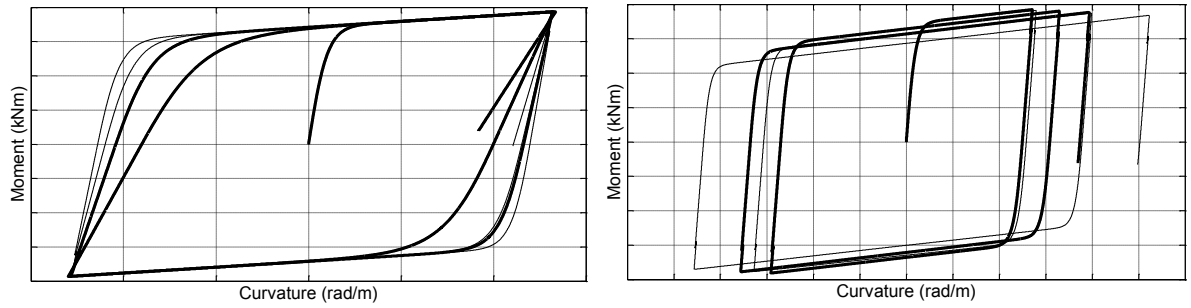

(a) (b)

Figure 4: Response for different values of c_n (a) and c_v (b) for sinusoidal excitation.

To account for pinching Foliente (1995) followed a similar approach to Baber and Wen by introducing an additional function *h(z)* in the basic differential equation that controls pinching:

$$\dot{z}(t)=h\left\{1-v_s\left|\frac{z}{z_y}\right|^n(\beta+\gamma sgn(z\dot{\varphi}))\right\}\frac{\dot{\varphi}}{n_s} \tag{10}$$

where *h* is defined as:

$$h = h\left(z, sgn\left(du\right), e\right) = 1 - \zeta_1 \exp\left(-\frac{\left(zsgn\left(du\right) - qz_u\right)^2}{\zeta_2^{\,2}}\right) \tag{11}$$

$$z_u = z_u\left(e\right) = \left(\frac{1}{\nu_s\left(\beta + \gamma\right)}\right)^{\frac{1}{n}} \tag{12}$$

$$\begin{aligned} \zeta_1 &= \zeta_1\left(e\right) = \zeta_{1,0}\left(1 - exp\left(-pe\right)\right) \\ \zeta_2 &= \zeta_2\left(e\right) = \left(\psi_0 + \delta_\psi e\right)\left(\lambda + \zeta_1\left(e\right)\right) \end{aligned} \tag{13}$$

Regarding the parameters introduced in the above equations (11), (12) and (13): p is a constant that controls the rate of initial drop in slope, $\zeta_{1,0}$ is the measure of total slip, ψ_0 is a parameter that contributes to the amount of pinching, $\delta\psi$ is a constant specified for the desired rate of pinching, λ parameter that controls the rate of change of ζ_2 as ζ_1 changes, q is a constant that sets a fraction of z_u as the pinching level, ζ_1 controls the intensity of pinching or magnitude of initial drop in slope (dz/du) and finally ζ_2 causes the pinching region to spread[5]. The pinching effect is shown in Figure 5.

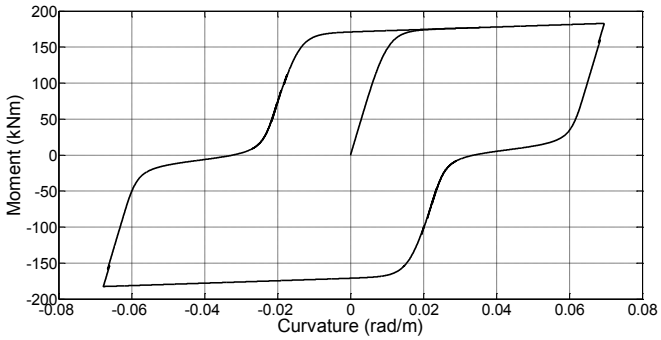

Figure 5: Response of cross section exhibiting pinching under sinusoidal excitation.

5 THE DETERIORATING HYSTERETIC BEAM ELEMENT

5.1 Constitutive relations

A prismatic 2d hysteretic beam element with start node 1 and end node 2, together with its end forces is presented in Figure 6.

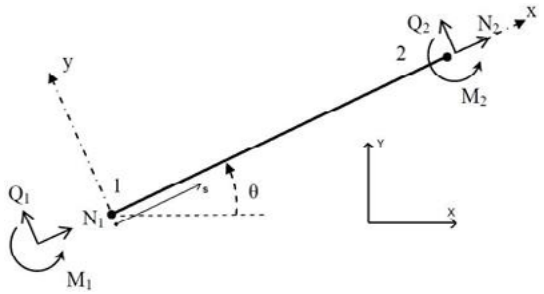

Figure 6: Hysteretic beam element

The inelastic moment-curvature relation and axial force-axial centerline strain relation at a cross section at a distance s from the start node are expressed as follows:

$$\begin{aligned} M(s,t) &= aEI\varphi(s,t) + (1-a)EIz(s,t) \\ N(s,t) &= a_u EAu(s,t) + (1-a_u)EAz_u(s,t) \end{aligned} \tag{14}$$

where M is the internal moment, φ is the total curvature, E is Young's modulus and I is the moment of inertia of the cross section, while N is the axial force and A the area of the cross section. The hysteretic parameter z is defined as the hysteretic part of the curvature when considering the bending degrees of freedom and z_u is the hysteretic axial centerline deformation. Introducing the evolution equations defined in (10) the following equations are obtained:

$$\begin{aligned} \dot{z}(t) &= h\left\{1 - v_s\left|\frac{z}{z_y}\right|^n (\beta + \gamma sgn(z\dot{\varphi}))\right\}\frac{\dot{\varphi}}{n_s} \\ \dot{z}_u(t) &= h_u\left\{1 - v_{s,u}\left|\frac{z_u}{\varepsilon_{0y}}\right|^n (\beta + \gamma sgn(z\dot{\varepsilon}_0))\right\}\frac{\dot{\varepsilon}_0}{n_{s,u}} \end{aligned} \tag{15}$$

Parameters α and α_u are material dependent that can be identified by independent pure bending and axial tests respectively.

Considering Euler-Bernoulli assumptions the curvature is approximated by the following relation:

$$\varphi = \frac{\partial^2 w}{\partial s^2} \tag{16}$$

where w is the transverse deflection of the beam. Substituting relation (16) into (14):

$$\begin{aligned} M(s,t) &= EI\tilde{\varphi}(s,t) \\ \tilde{\varphi}(s,t) &= a\frac{\partial^2 w(s,t)}{\partial s^2} + (1-a)z(s,t) \end{aligned} \tag{17}$$

where $\tilde{\varphi}(s,t)$ can be regarded as a measure of an "equivalent generalized curvature". Similarly considering the axial degrees of freedom we obtain:

$$\begin{aligned} N(s,t) &= EA\tilde{\varepsilon}_0(s,t) \\ \tilde{\varepsilon}_0(s,t) &= a_u\frac{\partial u(s,t)}{\partial s} + (1-a_u)z_u(s,t) \end{aligned} \tag{18}$$

where N is the axial force and $\tilde{\varepsilon}_0(s,t)$ is the generalized axial centerline strain in accordance with the generalized curvature $\tilde{\varphi}(s,t)$.

5.2 Discretization with Finite Element Method

Using cubic polynomial interpolation functions for the displacement field the following expression is derived:

$$\begin{bmatrix} u \\ w \end{bmatrix} = \begin{bmatrix} N_1 & 0 & 0 & N_2 & 0 & 0 \\ 0 & N_3 & N_4 & 0 & N_5 & N_6 \end{bmatrix} \{d\} \tag{19}$$

Where the nodal displacement vector *{d}* is defined as:

$$\{d\} = \{u_1 \quad w_1 \quad \theta_1 \quad u_2 \quad w_2 \quad \theta_2\}^T \tag{20}$$

while the corresponding shape functions are:

$$\begin{gathered} N_1 = 1 - \frac{s}{L} \qquad N_2 = \frac{s}{L} \qquad N_3 = 1 - \frac{3s^2}{L^2} + 2\frac{s^3}{L^3} \\ N_4 = s - \frac{2s^2}{L} + \frac{s^3}{L^2} \quad N_5 = \frac{3s^2}{L^2} - 2\frac{s^3}{L^3} \qquad N_6 = -\frac{s^2}{L} + \frac{s^3}{L^2} \end{gathered} \tag{21}$$

The total curvature φ can be expressed as:

$$\varphi = \begin{bmatrix} 0 & N_{3,ss} & N_{4,ss} & 0 & N_{5,ss} & N_{6,ss} \end{bmatrix} \{d\} = \begin{bmatrix} B_b(s) \end{bmatrix} \{d\} \tag{22}$$

where the subscript *,ss* denotes double differentiation with respect to the space variable s, which results in:

$$\varphi(s) = \begin{bmatrix} 0 & -\frac{6}{L^2} + \frac{12s}{L^3} & -\frac{4}{L} + \frac{6s}{L^2} & 0 & \frac{6}{L^2} - \frac{12s}{L^3} & -\frac{2}{L} + \frac{6s}{L^2} \end{bmatrix} \{d\} = \begin{bmatrix} B_b(s) \end{bmatrix} \{d\} \tag{23}$$

The hysteretic curvature is defined via the following linear shape functions [1]:

$$\mathrm{N}_7 = 1 - \frac{s}{L} \quad N_8 = \frac{s}{L} \tag{24}$$

and can be written as:

$$z_\varphi = \begin{bmatrix} N_7 & N_8 \end{bmatrix} \begin{Bmatrix} z_1^b \\ z_2^b \end{Bmatrix} = \begin{bmatrix} N \end{bmatrix}_z^b \begin{Bmatrix} z_1^b \\ z_2^b \end{Bmatrix} \tag{25}$$

the generalized curvature can therefore be expressed as:

$$\tilde{\varphi} = a \begin{bmatrix} 0 & N_{3,ss} & N_{4,ss} & 0 & N_{5,ss} & N_{6,ss} \end{bmatrix} \{d\} + (1-a) \begin{bmatrix} N_7 & N_8 \end{bmatrix} \begin{Bmatrix} z_1^b \\ z_2^b \end{Bmatrix} \tag{26}$$

Similarly the generalized centerline axial deformation is expressed as:

$$\tilde{\varepsilon}_0 = a \begin{bmatrix} N_{1,s} & 0 & 0 & N_{2,s} & 0 & 0 \end{bmatrix} \{d\} + (1-a) \begin{bmatrix} N_9 & N_{10} \end{bmatrix} \begin{Bmatrix} z_1^u \\ z_2^u \end{Bmatrix} \tag{27}$$

where the corresponding shape functions are[1]:

$$N_9 = -\frac{1}{L} \quad N_{10} = \frac{1}{L} \tag{28}$$

5.3 Constitutive matrix relation

By means of the principle of virtual work the following relation is obtained [1]:

$$\begin{bmatrix} \frac{a_u EA}{L} & 0 & 0 & -\frac{a_u EA}{L} & 0 & 0 & \frac{-(1-a_u)EA}{2} & \frac{-(1-a_u)EA}{2} & 0 & 0 \\ 0 & \frac{12aEI}{L^3} & \frac{6aEI}{L^2} & 0 & -\frac{12aEI}{L^3} & \frac{6aEI}{L^2} & 0 & 0 & -\frac{(1-a)EI}{L} & \frac{(1-a)EI}{L} \\ 0 & \frac{6aEI}{L^2} & \frac{4aEI}{L} & 0 & -\frac{6aEI}{L^2} & \frac{2aEI}{L} & 0 & 0 & -(1-a)EI & 0 \\ -\frac{a_u EA}{L} & 0 & 0 & \frac{a_u EA}{L} & 0 & 0 & \frac{-(1-a_u)EA}{2} & \frac{-(1-a_u)EA}{2} & 0 & 0 \\ 0 & -\frac{12aEI}{L^3} & -\frac{6aEI}{L^2} & 0 & \frac{12aEI}{L^3} & -\frac{6aEI}{L^2} & 0 & 0 & \frac{(1-a)EI}{L} & -\frac{(1-a)EI}{L} \\ 0 & \frac{6aEI}{L^2} & \frac{2aEI}{L} & 0 & -\frac{6aEI}{L^2} & \frac{4aEI}{L} & 0 & 0 & 0 & (1-a)EI \end{bmatrix} \begin{Bmatrix} \{d\} \\ \{z_u\} \\ \{z_b\} \end{Bmatrix} = \begin{Bmatrix} N_1 \\ Q_1 \\ M_1 \\ N_2 \\ Q_2 \\ M_2 \end{Bmatrix} \tag{29}$$

Relation (29) includes the elastic and hysteretic behavior of the element, where the axial forces are uncoupled with bending moments and shearing forces in both the elastic and hysteretic part. Additionally it can be written in a more compact form as:

$$\{\mathrm{f}\} = a[k]\{d\} + (1-a)[h]\{z\} \tag{30}$$

where the first term represents an elastic behavior based on the reduced, plastic stiffness and the second term adds the hysteretic part. It is evident that in the case where $a=a_u=1$ relation (29) reduces to the classical stiffness matrix of the elastic beam and the hysteretic term is wiped out. In relation (30) [k] is the element stiffness matrix and [h] is the element hysteretic matrix. These basic matrices are defined at elemental level, are formed once in the beginning of the analysis and remain unchanged thereafter.

5.4 Transformation to the global system

The end displacements of the element as well as the end forces can be expressed in the global system using the following relations:

$$\begin{aligned} \{d\} &= [\Lambda]\{u\} \\ \{F\} &= [\Lambda]\{\mathrm{f}\} \end{aligned} \tag{31}$$

where [Λ] is the classic 2D transformation matrix and θ is the right hand angle between the global X axis and the local x axis of the element (Figure 6). Consequently equation (30) can be written for both axial and bending components as:

$$\{F\} = a[\Lambda]^T[k][\Lambda]\{u\} + (1-a)[\Lambda]^T[h]\{z\} \tag{32}$$

5.5 Evolution equations

The nonlinear behavior of the element is governed by the Bouc-Wen evolution equations (10) including stiffness, strength degradation and pinching. Equations (15) using (22) transformed to the global system (32) can be expressed in terms of nodal velocities as:

$$\dot{z}_b(s,t) = h\left(1 - v_s\left|\frac{z(s,t)}{z_y}\right|^n \left(\beta + \gamma sgn\left(z(s,t)[B_b(s)][\Lambda]\{\dot{u}\}\right)\right)\right)[B_b(s)][\Lambda]\frac{\{\dot{u}\}}{n_s} \tag{33}$$

$$\dot{z}_u(s,t) = h_u\left(1 - v_{s,u}\left|\frac{z_u(s,t)}{z_y}\right|^n \left(\beta + \gamma sgn\left(z_u(s,t)[B_u(s)][\Lambda]\{\dot{u}\}\right)\right)\right)[B_u(s)][\Lambda]\frac{\{\dot{u}\}}{n_{s,u}} \tag{34}$$

5.6 State space formulation

The equation of motion for a frame structure with n_f degrees of freedom and n_{el} elements can be established as follows:

$$[M]_s\{\ddot{U}\}+[C]_s\{\dot{U}\}+[K]_s\{U\}+[H]_s\{Z\}=\{P(t)\} \tag{35}$$

where $[M]_s$ is the mass matrix, $[C]_s$ is the viscous damping matrix, $[K]_s$ is the stiffness matrix, containing only the elastic part of relation (30), $[H]_s$ is the hysteretic matrix of the structure and $\{P(t)\}$ is the (n_f x1) vector of external forces. The mass, viscous damping and the stiffness matrices are square symmetric with dimensions (n_f x n_f) while $[H]_s$ is orthogonal (n_f x $4n_{el}$). These matrices are assembled following the direct stiffness method, Bathe (2007) [7], while the viscous damping matrix in general may be of the form of a Rayleigh damping matrix, Chopra (2006) [8]. The unknown vectors {U} and {Z}, dictate the structure of the hysteretic matrix. The hysteretic behavior is defined at the element level in terms of hysteretic curvatures and centerline axial deformations from relations (33) and (34). The hysteretic matrix of each element, expressed in the global system, is appended to form the corresponding hysteretic matrix of the structure. Equations (35), together with evolution equations (33), (34), fully describe the response of the system to a given external force and initial conditions.

To solve the dynamic equilibrium equations presented in (35), the system can be transformed into a set of first order differential equations in state space form. Introducing the vector of nodal velocities $\{\dot{u}\}$ as auxiliary unknown vector we can write the system in a non-autonomous state-space form as follows:

$$\{\dot{x}\}=G(\{x\})+\{P(t)\} \tag{36}$$

where the vector {x} is defined as:

$$\{x\}^T=\begin{bmatrix}\{U\}^T & \{\dot{U}\}^T & \{Z\}^T\end{bmatrix} \tag{37}$$

and the operator G is:

$$G(\{x\})=\begin{bmatrix}0 & I & 0\\ [M]^{-1}[K] & [M]^{-1}[C] & [M]^{-1}[H]\\ 0 & Y(\{\dot{U}\},\{Z\}) & 0\end{bmatrix} \tag{38}$$

The operator G is a state dependent operator since Y contains the evolution equations of every element:

$$Y_j^i\left(\{\dot{u}\}^i,\{z\}^i\right)=h\left(1-v_s\left|\frac{z_j(t)}{z_y}\right|^n\left(\beta+\gamma\,\mathrm{sgn}\left(z_j(t)[B]_j[\Lambda]\{\dot{u}\}\right)\right)\right)[B]_j[\Lambda]\frac{\{\ddot{u}\}^i}{n_s} \tag{39}$$

The above system, for specific dynamic loading and given initial conditions on {x}, is integrated using a variable-order solver based on the numerical differentiation formulas (NDFs) i.e. a multistep solver.

6 NUMERICAL RESULTS

To verify the proposed model effectiveness in simulating the hysteretic behaviour of structural members its results are compared to existing experimental data. The material properties, the geometry of the specimen and a discussion of the experimental results are available in the study of T.Ninakawa and K.Sakino[9]. For the simulation one element was used and the results are shown in Figure 7. The parameters used for the model are $a=0.01$, $\beta=\gamma=0.5$, $n=2$, $c_n=0.005$, $c_v=0.003$, $\zeta_{1,0}=0.9$, $\rho=2$, $\psi_0=0.0215$, $\delta\psi=0.0003$, $\lambda = 0.3$, $q=0.02$.

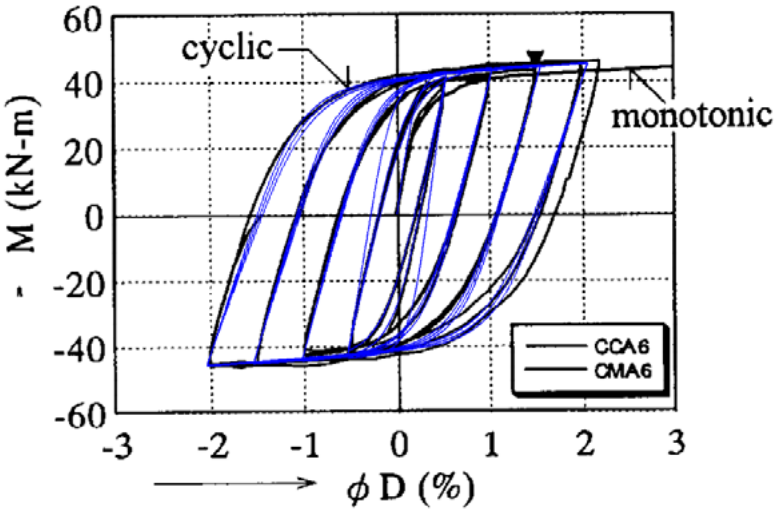

Figure 7: Analytical and experimental response of specimen CCA-6: Moment-Curvature diagrams

In the next example a typical 6 story frame (the Woodland Hills hospital in California) is subjected to the El Centro accelerogram, scaled up by a factor of 2. The geometry of the frame and its properties can be found in the work of Wong & Yang (1999)[10]. The results obtained for the left end section of the beam #25 of the first floor for the analysis without degradations are shown in Figure 8(a) while the results with degradations are shown in Figure 8(b).

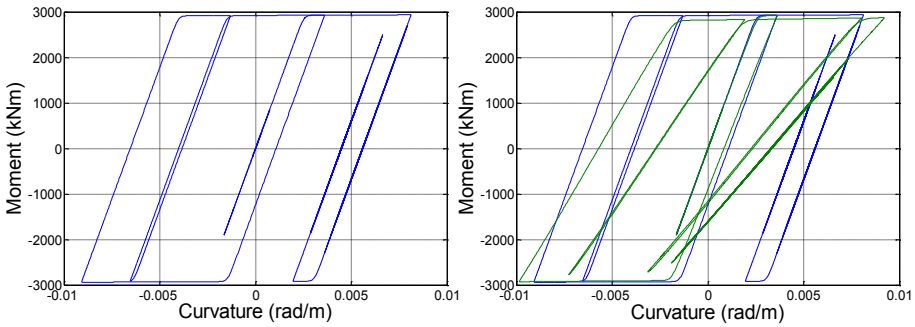

Figure 8: Moment-Curvature diagram for the end section of beam #25 without degradations (a) and with degradations(b).

CONCLUDING REMARKS

A wide range of hysteretic behavior can be modeled by the proper control of the Bouc-Wen model parameters and the degradation parameters. The beam element is formulated with four new degrees of freedom accounting for the hysteretic part of the curvature and axial centerline deformation. The entire problem is casted into two sets of equations namely the linear equations of motion and the nonlinear evolution equations, which are solved simultaneously by implementing a numerical differentiation scheme. Comparisons between the results and experimental data show good correlation demonstrating the effectiveness of the proposed model to simulate degradation effects.

REFERENCES

[1] Triantafyllou, S. and Koumousis, V. Small and large displacement analysis of frame structures based on hysteretic beam elements. *Journal of Engineering Mechanics ASCE*, **138**:36-49, (2012).

[2] Baber, T.T. and Wen, Y.K. Random vibration of hysteretic degrading systems. *Journal of the Engineering Mechanics Division, Proc. ASCE*, **107(6)**:1069-1087, (1981).

[3] Foliente, G.C., Hysteresis Modelling of Wood Joints and Structural Systems. *Journal of Structural Engineering , ASCE*, **121(6)**:1013-1022, (1995).

[4] Wen, Y.-K. Equivalent linearization for hysteretic system under random excitation, *Journal of Applied Mechanics*, **47**:150-154, (1980).

[5] Ma, Ma F. Zhang, H. Bockstedte A. Foliente, G.C. Paevere P. Parameter analysis of the differential model of hysteresis, *Journal of Applied Mechanics ASME*, **71**:342– 349, (2004).

[6] Wang, C. Foliente, G.C. Hysteretic Models For Deteriorating Inelastic Structures, *J. Engrg. Mech.,ASCE,***127(11)**:1200-1202, (2001).

[7] Bathe K.J., 2007, Finite Element Procedures, *Prentice Hall Engineering*, Science, Mathematics, New York.

[8] Chopra A., "Dynamics of Structures", 2006, *Prentice Hall*, New York.

[9] T.Ninakawa, K. Sakino, Inelastic behavior of concrete filled circular steel tubular columns subjected to uniform cyclic bending moment, Eleventh World Conference on Earthquake engineering, 1358,(1996).

[10] Wong K., Yang Ron, "Inelastic Dynamic Response of Structures Using Force Analogy Method", *Journal of Engineering Mechanics*, Vol. 125, No. 10.1999.

[11] Baber, T. T, Noori, M. -N (1985) "Random vibration of degrading pinching systems "*,Journal of the Engineering Mechanics* Division,Proc. ASCE, 11(8):1010-1026

[12] Sivaselvan, M. V, Reinhorn, A. M (2000) "Hysteretic Models For Deteriorating Inelastic Structures", *J. Engrg. Mech*. ,ASCE,126(6):633-640

[13] Takeda, T., Sozen, M.A., Nielsen, N.N. (1970) "R/C response to simulated earthquakes", Am. Soc. Civ. Engrs, *J. Struct*. Div., 96(ST12):2557-2573.

[14] Park, Y.J., Reinhorn, A.M., Kunnath, S.K. (1987) "IDARC: Inelastic damage analysis of reinforced concrete frame-shear wall structures", *National Center for Earthquake Engineering Research*, State University of New York, Buffalo, NY, Tech. Rep. NCEER-87- 0008.